A Crossed Molecular Beam Study of the $O(^1D) + C_3H_8$ Reaction: Multiple Reaction Pathways

Jinian Shu,[†] Jim J. Lin,[†] Yuan T. Lee,[†,‡] and Xueming Yang*[,§,||]

Contribution from the Institute of Atomic and Molecular Sciences, Academia Sinica, Taipei, Taiwan, Department of Chemistry, National Taiwan University, Taipei, Taiwan, and Department of Chemistry, National Tsing Hua University, Hsinchu, Taiwan

Received September 21, 2000

Abstract: The $O(^1D) + C_3H_8$ reaction has been reinvestigated using the universal crossed molecular beam method. Three reaction channels, $CH_3 + C_2H_4OH$, $C_2H_5 + CH_2OH$, and $OH + C_3H_7$, have been observed. All three channels are significant in the title reaction with the C_2H_5 formation process to be the most important, while the CH_3 formation and the OH formation channels are about equal. Product kinetic energy distributions and angular distributions have been determined for the three reaction channels observed. The oxygen-containing radicals in the CH_3 and C_2H_5 formation pathways show forward−backward symmetric angular distribution relative to the O atom beam, while the OH product shows a clearly forward angular distribution. These results indicate that the OH formation channel seems to exhibit different dynamics from the CH_3 and C_2H_5 channels.

1. Introduction

Experimental investigations of chemical kinetics of multiple pathway reactions are important in atmospheric chemistry and combustion processes. However, modern experimental studies of reaction dynamics have been largely focused on elementary bimolecular reactions during the last few decades. Complicated reactions of energetic species with multiple reaction channels have received little attention. This is due largely to the lack of more sensitive universal detection methods for chemical reaction products. Accurate theoretical dynamical calculations for complicated reactions are still lacking even though the field of theoretical chemistry has grown tremendously during the last two decades.

The universal crossed molecular beam technique based on electron impact ionization has been essential in investigating the dynamics of bimolecular chemical reactions during the last few decades. Product angular and kinetic energy distributions can be measured using this powerful method.[1,2] Electron impact ionization with quadrupole mass selection is, in principle, an ideal universal detection method for all reaction products. The detection efficiency of this method is, however, limited by the low quadrupole transmission efficiency, the low ionization efficiency, and the high background in the detector. Recently, a new apparatus has been set up with much improved detection efficiency and aims to study more complicated chemical reactions.[3] A custom-designed, larger-sized quadrupole mass filter was installed in an effort to increase the transmission efficiency for product ions. Much lower background in the detector ($<10^{-12}$ Torr) has also been achieved using multiple ultrahigh vacuum pumps and cleaner vacuum conditions. With these efforts, the detection efficiency is much improved for all reaction products. This improved instrument provides a new tool for investigating the dynamics of more complex reactions with multiple pathways under a single collision condition.

The reactions of $O(^1D)$ with small alkanes have been studied extensively during the last few decades.[4−15] Among those reactions, the reaction with methane is the most important since methane is the most abundant hydrocarbon in the atmosphere. The reaction of methane with $O(^1D)$ is an important source for stratospheric OH, and that oxidation is also a source of a portion of stratospheric H_2O, which itself is a source of OH through reaction with $O(^1D)$. The OH radical generated from this source partly determines the chemistry of the earth's ozone layer through the HO_x cycles.[16,17] Furthermore, this reaction also plays a significant role in tropospheric chemistry. In addition to the $CH_3 + OH$ channel, there are also other significant channels in the $O(^1D)$ reaction with methane, such as the atomic hydrogen formation channel ($H + H_3CO/H_2COH$) and the molecular hydrogen formation channel ($H_2 + H_2CO/HCOH$).[18−20] Even

[†] Institute of Atomic and Molecular Sciences, Academia Sinica.
[‡] National Taiwan University.
[§] National Tsing Hua University.
[||] JILA visiting Fellow, JILA, University of Colorado at Boulder, Boulder, CO 80309-0440. E-mail: xmyang@po.iams.sinica.edu.tw.

(1) Lee, Y. T.; McDanald, J. D.; Lebreton, P. R.; Hershbach, D. R. *Rev. Sci. Instrum.* **1969**, *40*, 1402.
(2) Lee, Y. T. *Science* **1987**, *236*, 793−798.
(3) Lin, J. J.; Hwang, D. W.; Lee, Y. T.; Yang, X. *Rev. Sci. Instrum.* **1998**, *69*, 1642.
(4) Yamazaki, H.; Cvetanovic, R. J. *J. Chem. Phys.* **1964**, *41*, 3703.
(5) Michaud, P.; Cvetanovic, R. J. *J. Phys. Chem.* **1972**, *76*, 1375.
(6) Parakevopoulos, G.; Cvetanovic, R. J. *J. Chem. Phys.* **1969**, *50*, 590.
(7) Parakevopoulos, G.; Cvetanovic, R. J. *J. Chem. Phys.* **1970**, *52*, 5821.
(8) Lin, C. L.; DeMore, W. B. *J. Phys. Chem.* **1973**, *77*, 863.
(9) DeMore, W. B.; Raper, O. F. *J. Chem. Phys.* **1967**, *46*, 2500.
(10) Jayanty, R.; Simonaitis, R.; Heicklen, J. *Int. J. Chem. Kinet.* **1976**, *8*, 10.
(11) Casavecchia, P.; Buss, R. J.; Sibbener, S. J.; Lee, Y. T. *J. Chem. Phys.* **1980**, *73*, 6351.
(12) Satyapal, S.; Park, J.; Bersohn, R.; Katz, B. *J. Chem. Phys.* **1980**, *91*, 6873.
(13) Aker, P. M.; Obrien, J. J. A.; Sloan, J. J. *J. Chem. Phys.* **1986**, *84*, 745.
(14) Cheskis, S. G.; Iogansen, A. A.; Kulakov, P. V.; Razuvaev, I. Y.; Sarkisov, O. M.; Titov, A. A. *Chem. Phys. Lett.* **1989**, *155*, 37.
(15) Park, C. R.; Wiesenfeld, J. R. *J. Chem. Phys.* **1991**, *95*, 8166.
(16) Brasseur, G.; Solomon, S. *Aeronomy of the Middle Atmosphere*; Reidle: Boston, 1984.
(17) Wiesenfeld, J. R. *Acc. Chem. Res.* **1982**, *15*, 110.
(18) Lin, J. J.; Lee, Y. T.; Yang, X. *J. Chem. Phys.* **1998**, *109*, 2975.
(19) Lin, J. J.; Harich, S.; Lee, Y. T.; Yang, X. *J. Chem. Phys.* **1999**, *110*, 10821.

10.1021/ja003456p CCC: $20.00
Published on Web 12/15/2000

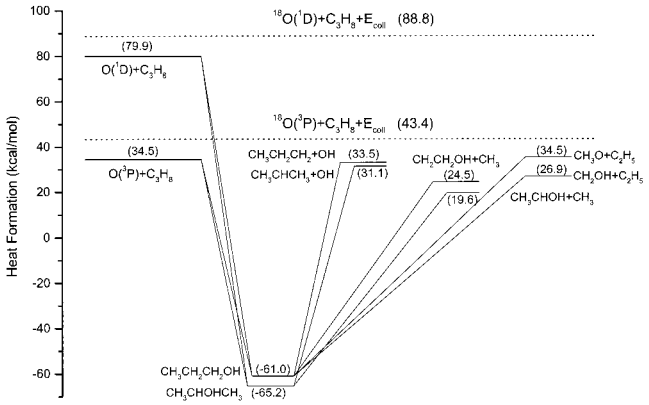

Figure 1. Energy diagram for possible reaction channels of the bimolecular reaction of $O(^1D) + C_3H_8$. The numbers in the parentheses are the energies in kcal/mol.

though the reaction of $O(^1D)$ with CH_4 is well studied, reactions of $O(^1D)$ with other alkane molecules have rarely been studied carefully. These reactions could have some implications in atmospheric chemistry since alkanes have relatively long lifetimes and could actually produce different radicals at different altitudes in the atmosphere where OH formation from the $O(^1D) + H_2O$ reaction is becoming less important and OH formation from other sources, such as $O(^1D) + CH_4$, are more important. Therefore it would be interesting to know the relative branching ratios of the OH formation channel in the $O(^1D)$ + alkane reactions.

It is well-known that many reactions of $O(^1D)$ go through insertion mechanisms, in which long-lived intermediates are normally formed. For example, the $O(^1D) + H_2 \rightarrow OH + H$ reaction is a typical insertion chemical reaction at low collisional energies (less than ~2 kcal).[21,22] However, recent experimental studies show that that the $O(^1D)$ reaction with H_2 also occurs via an abstraction mechanism at larger collisional energies (larger than ~2 kcal/mol).[3] The reaction of $O(^1D)$ with methane is also interesting; multiple dynamical pathways have been discovered, while insertion is still likely the most important reaction mechanism. Therefore, it is interesting to understand how the reaction mechanism of the $O(^1D)$ reaction changes as the other reactant becomes larger. The OH channel for the $O(^1D)$ reactions with small alkanes have also been studied by Wiesenfeld et al.[15] Their results show that the yield of the OH formation channel in the $O(^1D)$ reactions with ethane and propane is much smaller than that in the $O(^1D)$ reaction with methane. Mechanism for this channel is also an interesting issue since some experimental evidence shows that the OH formation proceeds at least in part by a direct abstraction mechanism.[4−10,13,14] However, experimental results by Wiesenfeld et al.[15] show that a long-lived complex should be responsible for the OH formation channel. Recently, we have initiated a series of studies on the $O(^1D)$ reaction with small alkanes using our improved crossed beam appratus to try to better understand the mechanism of this reaction. The results of the $O(^1D)$ reaction with propane are reported here.

Figure 1 shows the energy diagram for all possible reaction channels for the bimolecular reaction $O(^1D) + C_3H_8$. The energetics shown in Figure 1 were calculated on the basis of previous experimental and theoretical results.[23−31] From the energetics, it is clear that many reaction channels or microchannels are energetically accessible for the title reaction. It is therefore interesting to understand the dynamics of this complicated reaction. In this work, crossed molecular beam studies on this reaction were carried out. By both careful measurements and detailed analyses of the TOF spectra and angular distributions of products from the crossed molecular beam study of the $O(^1D) + C_3H_8$ reaction, a more complete dynamical picture of this reaction is presented.

2. Experimental Methods

The reaction of O atom with C_3H_8 has been studied recently in our laboratory using the crossed molecular beam techniques. The apparatus used in this experiment is a newly built crossed molecular beam machine which has been described in detail elsewhere.[3] Briefly, the oxygen atomic beam, generated using the photodissociation of O_2 at 157.6 nm in a skimmed O_2 pulsed beam, was crossed with a skimmed C_3H_8 beam at a fixed angle of 90°. The O_2 beam was obtained by expanding a neat O_2 (99.99%) sample through a commercial pulsed valve (General Valves) with a rise time of about 50 μs, at a stagnation pressure of about 5 atm. The molecular beam was then skimmed by a sharp-edged skimmer (Beam Dynamics) with 2 mm diameter orifice. The O_2 beam was then intercepted by a 157.6 nm laser beam, generated by a Lambda Physik LPX210I F_2 laser, with pulse energy of about 30 mJ at a repetition rate of 50 Hz. Both $O(^1D)$ and $O(^3P)$ were generated in the 157 nm photolysis of O_2 with a ratio of 50:50. The $O(^3P, ^1D)$ beam was then skimmed once before entering the main chamber to cross the propane beam. To reduce the O_2 background both in the main chamber and in the detector, the O_2 beam was rotated to some angle from the detector plane. By setting O_2 beam to different angles, different beam velocities of the O beam could be obtained. The F_2 laser beam was focused to a spot of 4 mm(w) × 4 mm(h) in the interaction region by a spherical-cylindrical MgF_2 shaping lens. By using the above focusing condition and laser power, the O_2 transition (cross-section $s = 6.8 \times 10^{-18}$ cm^2) at 157.6 nm can be easily saturated. The C_3H_8 molecular beam was generated by expanding a neat C_3H_8 sample at a stagnation pressure of 5 atm through a carefully adjusted pulsed valve (General Valve) with a rise time of about 60 μs and then skimmed once by a 1.5 mm orifice skimmer before entering the main chamber. The O atomic beam, the C_3H_8 molecular beam, and the detection axis are all in the same plane. The velocity spread of the O atomic beam is less than 2%. The collisional energy of the reaction is 8.0 kcal/mol in this experiment. The angular divergence of the O atomic beam was about ±3°. In this experiment, $^{18}O_2$ has been used to avoid the background from the detector and the propane beam. The speed of the C_3H_8 beam was about 820 m/s with a speed ratio of about 9 and an angular divergence of about ±2°. Reaction products scattered from the crossed region are detected by a mass-selective, electron impact ionization detector. The whole experiment was carried out in a pulsed mode, and time zero was defined as the time when the two beams were crossed. After flying about 25 cm from the crossed region, the neutral reaction products were then ionized by a Brink's-type electron impact ionizer with electron energy of about 60 eV. The product ions were mass-filtered by a quadrupole mass filter and counted by a Daly ion detector. All time-of-flight (TOF) spectra were taken at 1 μs per channel during the experiment. The TOF spectra shown in this work were all rebinned to 3 μs per channel for better S/N ratio without distorting the shape of the TOF spectra. The product angular distribution can also be measured by rotating the detector. During the experiments described

(20) Lin, J. J.; Shu, J.; Lee, Y. T.; Yang, X. *J. Chem. Phys.* **2000**, *113*, 5287.
(21) (a) Hsu, Y.-T.; Wang, J.-H.; Liu, K. *J. Chem. Phys.* **1997**, *107*, 1664. (b) Hsu, Y.-T.; Liu, K. *J. Chem. Phys.* **1997**, *107*, 2351.
(22) Liu, X.; Lin, J. J.; Harich, S. A.; Schatz, G. C.; Yang, X. *Science* **2000**, *289*, 1536.
(23) Espinosa-Garcia, J.; Olivares Del Valle, F. J. *J. Phys. Chem.* **1993**, *37*, 3377.
(24) Curtiss, L. A.; Kock, L. D.; Pople, J. *J. Chem. Phys.* **1991**, *95*, 4040.
(25) Tachikawa, H. *Chem. Phys. Lett.* **1993**, *212*, 27.
(26) Bauschlicher, C. W., Jr.; Partridge, H. *J. Phys. Chem.* **1994**, *98*, 1826.
(27) Cui, Q.; Morokuma, K. *Chem. Phys. Lett.* **1996**, *263*, 54.
(28) Walch, S. P. *J. Chem. Phys.* **1993**, *98*, 3163.
(29) Johnson, R. D., III; Hudgens, J. W. *J. Phys. Chem.* **1996**, *100*, 19874.
(30) Lin, M. C. Emory University, private communication.
(31) Walch, S. P. *J. Chem. Phys.* **1993**, *98*, 3076.

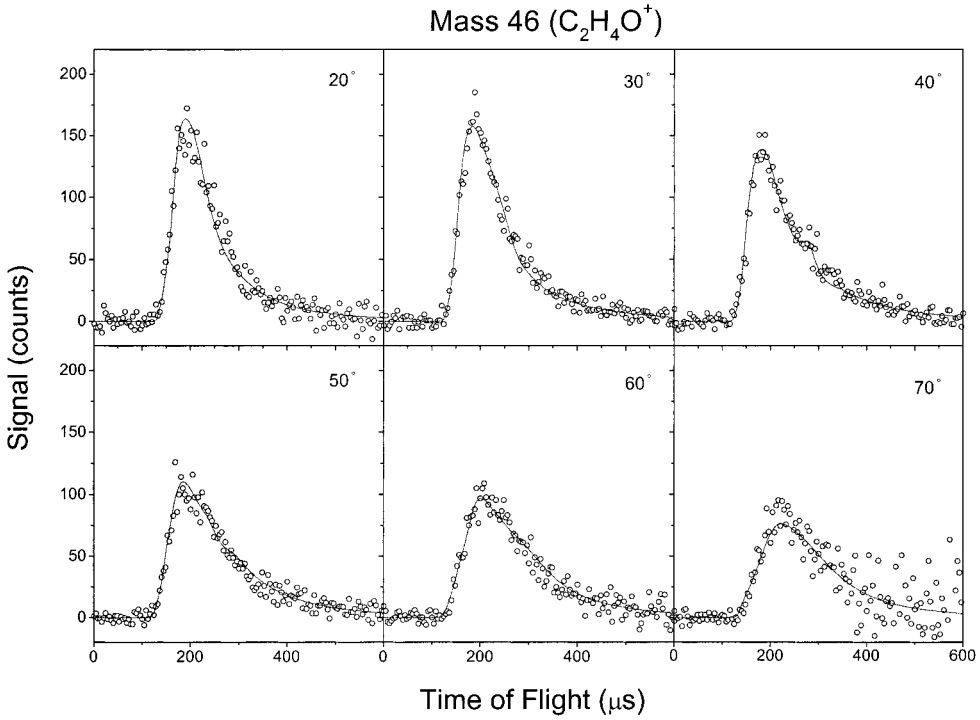

Figure 2. TOF spectra at mass 46 at six different laboratory angles. The open circles represent the experimental data, while the solid lines are the simulated results. Each experimental spectrum was obtained by accumulating signals over 250K laser shots.

above, the vacuum in the detector ionization region was maintained at 1×10^{-12} Torr. The time-of-flight spectra and angular distributions of the neutral products measured in the laboratory (LAB) frame were converted to the kinetic energy distributions and angular distributions in the center-of-mass (CM) frame by using a computer simulation program, which is capable of simulating multiple channel contributions in a crossed beam reaction.

3. Results and Discussion

3.1. CH_3 Formation Channel. TOF signals have been observed at mass 46 and mass 45 from the reaction $^{18}O + C_3H_8$. No such signal has been observed at higher masses. No signal at masses slightly lower than the mass of the reaction complex ($C_3H_8{}^{18}O$) has also been detected, indicating that there is H or H_2 loss channel in this reaction. The signal observed at mass 46 is likely from the CH_3 formation channel in which one of the two C−C bonds ruptures in the reaction complex, leaving likely a C_2H_5O radical. The parent signal at mass 47 is not observed in this case, which is probably caused by the total dissociative ionization of the parent radical. Figure 2 shows the experimental TOF spectra (in open circles) of the reaction product at mass 46. A signal at mass 46 is observed in the laboratory angle range of 20°−70°. The TOF spectra shown in Figure 2 are simulated using a computer program, assuming this is from the $CH_3 + C_2H_5O$ channel (a mass ratio of 15:47). Since the CM product kinetic angular distribution $P(E)$ is angular-dependent, several numerical $P(E)$ functions at different CM angles are necessary to model the whole angular-dependent product kinetic energy distribution by linear interpolation. $P(E)$ functions at other angles are linearly interpolated using the above $P(E)$ functions adjustable in the program. In the simulation of the CH_3 formation channel, four slightly different $P(E)$ functions were used. By adjusting these four $P(E)$ functions iteratively, the TOF spectra observed at different laboratory angles were be simulated. Product CM angular distribution was also obtained by iterative simulation to the TOF spectra. These distributions were adjusted numerically until satisfactory fits to all the TOF

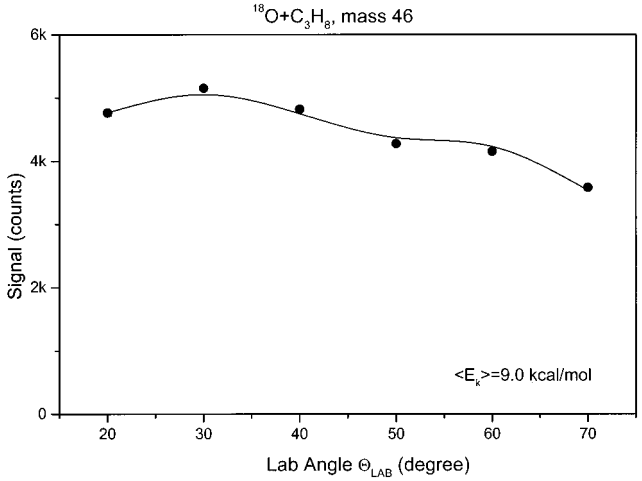

Figure 3. Laboratory angular distribution of product at mass 46. Open circles are the experimental data, while the sold line is the simulated results.

spectra and the laboratory product angular distribution are obtained. Figures 2 and 3 also show the simulated results (solid lines) that are in good agreement with the experimental data (open circles).

The CM kinetic energy distributions at three CM angles obtained from the above simulation are shown in Figure 4, while the CM product angular distribution is shown in Figure 5. From these distributions, a three-dimensional (3D) product flux diagram of the radical product from this CH_3 formation channel can be constructed, which is shown in Figure 6. From Figures 5 and 6, it is quite obvious that this product channel likely proceeds through a long-lived complex, which could be formed through an insertion reaction mechanism. From Figure 4, it is clear that the cutoff of the CM kinetic energy distributions are around 30 kcal/mol, which is much less than the available energies of two CH_3 formation microchannels: $CH_3CHOH + CH_3$ (69.2 kcal/mol) and $CH_2CH_2OH + CH_3$ (64.3 kcal/mol)

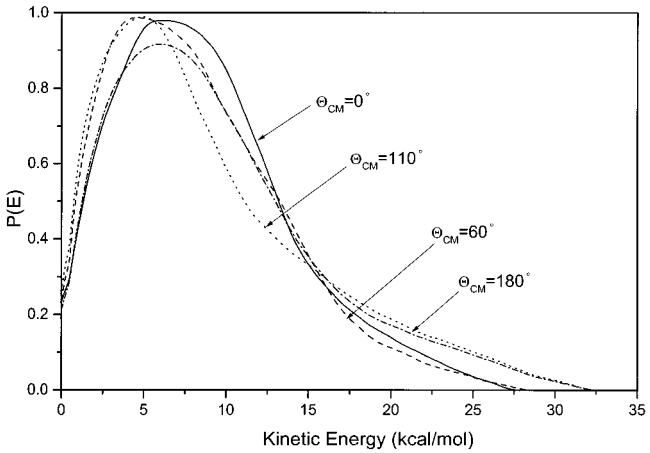

Figure 4. CM product kinetic energy distributions used in simulating the TOF spectra shown in Figure 2. Total of three distributions are used at three CM angles.

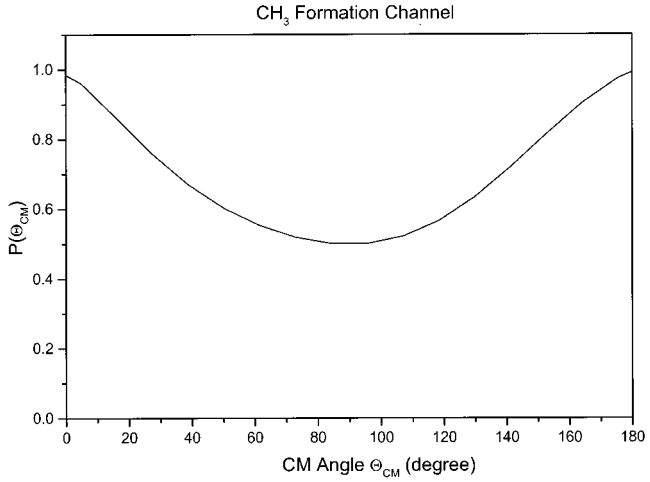

Figure 5. CM angular distribution of product observed at mass 46 obtained from simulating the TOF spectra (Figure 2) and the laboratory angular distribution (Figure 3).

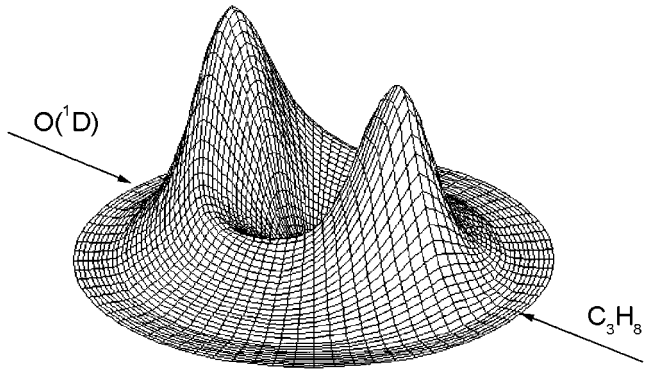

Figure 6. 3D product flux diagram (mass 46) constructed from the CM product kinetic energy distributions (Figure 4) and the CM angular distribution (Figure 5).

for the O(^{1}D) reaction. This is a quite common observation for reaction channels with two molecular products. Since the O(^{3}P) reaction is also energetically possible with about 20 kcal/mol available energy, its relative reactivity should be a concern in this work. It is known that the parent radical ion has not been observed in this reaction channel, therefore, the radical products from this channel must be quite hot, indicating that most of the reaction products are likely from the O(^{1}D) reaction. This is reasonable since energetically the O(^{3}P) reaction is less favorable than the O(^{1}D) reaction. For the two possible radical pathways, $CH_3CHOH + CH_3$ and $CH_2CH_2OH + CH_3$, it is not clear which one is more important. Energetically, both processes should be important. Even though the $CH_3CHOH + CH_3$ pathway is energetically more favorable than the $CH_2CH_2OH + CH_3$ pathway, it is dynamically harder to access since it clearly needs a hydrogen atom migration if the O atom is inserted into the C−H bonds at the two ends of propane, which is statistically a more likely process. The observation of the following C_2H_5 channel indicates that the O atom insertion at the two ends of propane is likely the more important process. If the O atom inserts into the middle C−H bonds, then the former process should be a dynamically favorable process. In any case, this is an interesting issue that needs further theoretical investigations.

3.2. The $C_2H_5 + CH_2OH$ Channel. Signals at mass 33 ($CH_3{}^{18}O^+$) have been observed from the $^{18}O + C_3H_8$ reaction. TOF spectra observed in the scattering angle of −5° to 110° have been measured carefully and are shown in Figure 7, with the experimental laboratory product angular distribution shown in Figure 8. From this relative large angular scattering range, it is quite clear that the masses of two partner products must be quite comparable. Since the TOF spectra observed at mass 33 are significantly different from those TOF spectra at mass 46 and mass 45, indicating that the signals observed at mass 33 is from a completely different reaction channel rather than from dissociative ionization of the radical product from the CH_3 formation channel. Therefore, another energetically possible channel, the C_2H_5 formation, is likely responsible for the signals observed at mass 33, which is the mass of the scattering partner (CH_2OH or CH_3O) of this reaction channel.

The TOF spectra were then simulated as the C_2H_5 formation channel with a product mass ratio of 29:33 using the same computer program with procedures similar to those used above. In this case, four $P(E)$ functions in the CM frame are used along with a single CM product angular distribution. The simulated results (solid lines) are shown in Figures 7 and 8 along with the experimental data (open circles). From these figures, it is clear that the agreement between the experimental data and simulated results are quite good. The translational energy distributions obtained from the simulating the experimental TOF spectra are shown in Figure 9. The four distributions at different CM angles are shown to be very similar to each other with the energy cutoff around 25 kcal/mol. The averaged kinetic energy release for this process is about 10 kcal/mol, while the available energy is about 62 kcal/mol for the $C_2H_5 + CH_2OH$ pathway and about 53 kcal/mol for the $C_2H_5 + CH_3O$ pathway, indicating that much of the available energy is deposited into the radical products. The fact that the cutoff energy observed is much smaller than the available energies of this channel is also an indication that much of the energy is deposited into the internal energy of the product. This is similar to that of the CH_3 channel. Clearly both of these two pathways are open in this channel. The radical product detected in this channel could either be methoxy radical (CH_3O) or hydroxymethyl radical (CH_2OH). From our previous experimental investigation[20] on the pattern of dissociative ionizations of these two radicals, CH_3O is known to be extremely unstable in an electron impact ionizer and would crack into $HCO^+ + H_2$ very readily. Therefore, the parent ion of CH_3O at mass 33 in this case should not exist, and the product observed at mass 33 in this experiment should come from hydroxymethyl radical only. This is not surprising since the $C_2H_5 + CH_2OH$ channel is energetically more favorable. The O(^{3}P) reaction could also occur. In the O(^{3}P) reaction, the two radical pathways for the C_2H_5 channel have available energies of 16

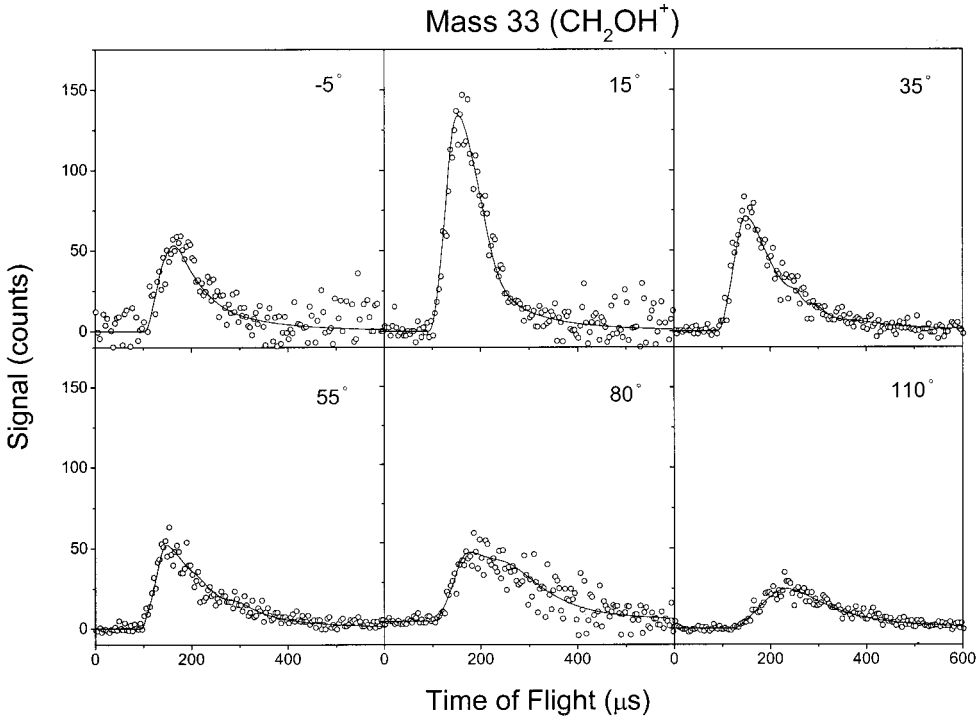

Figure 7. TOF spectra at mass 33 at nine different laboratory angles. The open circles represent the experimental data, while the solid lines are the simulated results. Each experimental spectrum was obtained by accumulating signals over 250K laser shots.

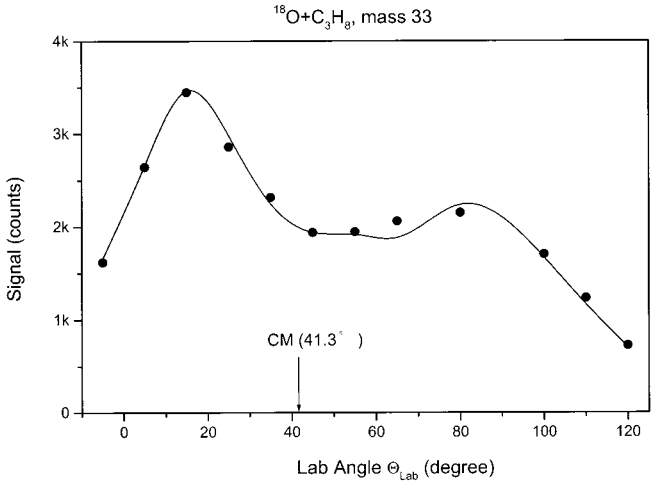

Figure 8. Laboratory angular distribution of product at mass 33. Open circles are the experimental data while the sold line is the simulated results.

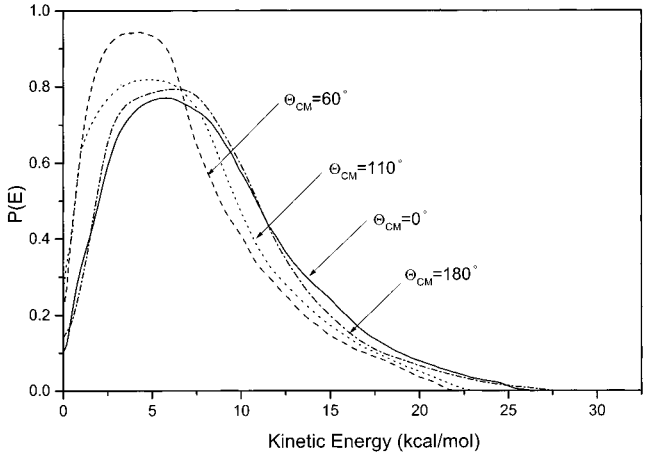

Figure 9. CM product kinetic energy distributions used in simulating the TOF spectra shown in Figure 7. Total of four distributions are used at four CM angles.

kcal/mol (CH_2OH) and 9 kcal/mol (CH_3O), which are significantly lower than the observed energy cutoff (25 kcal/mol). This implies that the majority of the products at mass 33 should come from the energetically more favorable $O(^1D)$ reaction.

The CM product angular distribution obtained from the above simulation is shown in Figure 10. From the CM translational energy distributions and the CM product angular distribution, a 3D product flux diagram for the radical product (hydroxymethyl radical) is constructed and shown in Figure 11. From these two figures, it is quite obvious that the hydroxymethyl radical is essentially scattered forward−backward symmetrically relative to the $O(^1D)$ atom beam, implying that this reaction channel likely occurs through a long-lived complex mechanism, similar to the CH_3 formation channel. Since hydroxymethyl radical is the major product in the reaction channel, it is quite likely that the long-lived reaction complex is formed through an insertion pathway in which the $O(^1D)$ atom inserts into a C−H bond of the propane molecules. It is also clear that the insertion site is more likely at the two ends rather than at the middle of the propane molecule since this is the only direct route to form a CH_2OH radical.

In addition to the signals observed at mass 33, TOF spectra at mass 31 have also been measured carefully, which are shown in Figure 12. The spectra at mass 31 are obviously more complex than the ones at mass 33. From careful fittings, all of these TOF spectra can be simulated by including all of the known channels, indicating that all signals at mass 31 comes from dissociative ionization of the radical products in the ionizer from the above two reaction channels. Figure 13 shows the contribution of each channel to the laboratory angular distribution of product at mass 31. These fittings are important to estimate the relative importance of each of the different channels in this reaction.

3.3. The OH + C_3H_7 Channel. OH radical product at mass 17 has been observed in the $O(^1D) + C_3H_8$ reaction. The small

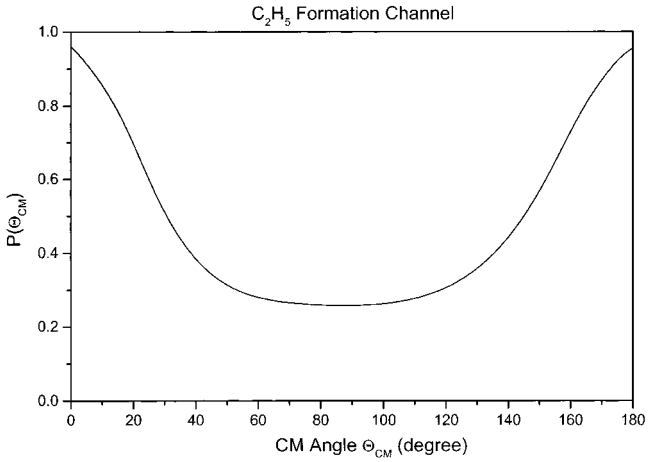

Figure 10. CM angular distribution of product observed at mass 33 obtained from simulating the TOF spectra (Figure 7) and the laboratory angular distribution (Figure 8).

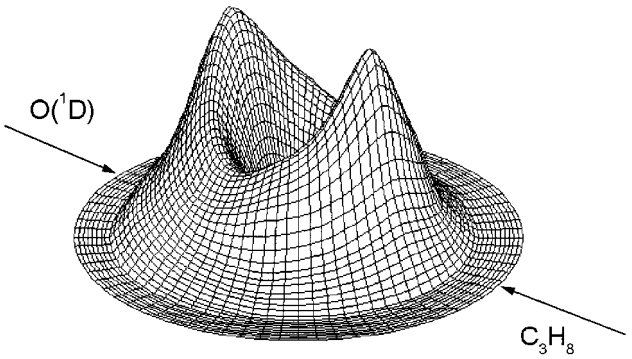

Figure 11. 3D product flux diagram (mass 33) constructed from the CM product kinetic energy distributions (Figure 9) and the CM angular distribution (Figure 10).

amount of OH^+ (mass 17) background from the residual detector H_2O background, $\sim 5 \times 10^{-14}$ Torr partial pressure, makes the experiment much harder if not impossible. To avoid these problems, $^{18}O_2$ is used to generate the $^{18}O(^1D)$ beam instead of normal O_2 as in the above channels. In this way, the product ^{18}OH should be at mass 19 where there is little interference from either the propane beam or the detector H_2O background.

Since the ^{18}OH radical is lighter than the C_3H_7 radicals, the kinetic energies carried by the OH radical products from the title reaction should be larger. Therefore, the OH products in this reaction channel should scatter into a large solid angle. TOF spectra at eleven laboratory angles (from $-5°$ to $120°$) have been measured in this experiment. Figure 14 shows the six TOF spectra (open circles) taken for the ^{18}OH product with the correct relative signals. By integrating the signal of each TOF spectra, the OH product angular distribution for this channel in the laboratory frame was also determined. Figure 15 shows the laboratory angular distribution of the ^{18}OH product. From the TOF spectra and the angular distribution measured in the laboratory frame, product kinetic energy distributions and product angular distributions in the center-of-mass frame can be determined using the same method as that described above. Since the CM product kinetic angular distribution $P(E)$ is angular-dependent, four numerical $P(E)$ functions at different CM angles were used in the simulation. The simulated results (solid lines) agree well with the experimental data (open circles) (see Figures 14 and 15). Figure 16 shows the CM product kinetic energy distributions obtained from simulating the TOF spectra at mass 19. Figure 17 shows the CM product angular distribution obtained from fitting the experimentally measured angular distribution. The simulated and experimental results are in good agreement with each other. From the above distributions, a 3D CM product flux diagram for the OH product, shown in Figure 18, was constructed. From Figures 17 and 18, one can see that the overall OH product is clearly forward-scattered relative to the $O(^1D)$ beam direction, indicating that the dynamics of the OH formation are quite different from those of the two observed channels described in the last sections, in which the radical

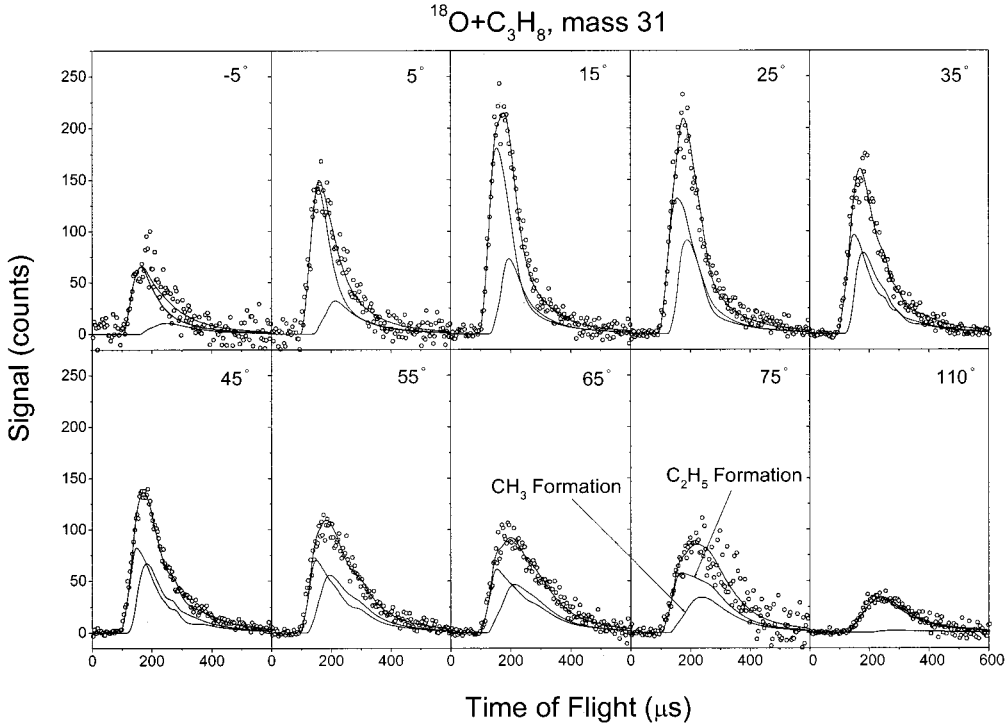

Figure 12. TOF spectra at mass 31 at six different laboratory angles. The open circles represent the experimental data, while the solid lines are the simulated results. Each experimental spectrum was obtained by accumulating signals over 250K laser shots. These results show multiple contributions from different reaction channels.

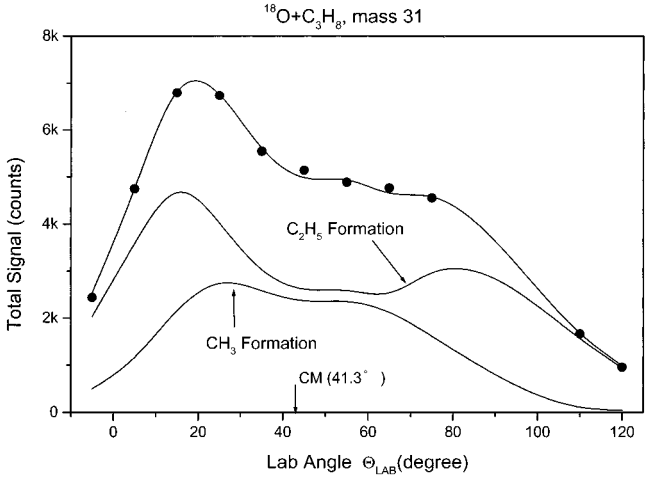

Figure 13. Laboratory angular distribution of product at mass 46. Open circles are the experimental data, while the sold line is the simulated results.

products all show forward−backward symmetric angular distribution. The averaged kinetic energy release for this channel is about 10 kcal/mol, indicating that most of the available energy in this channel is deposited into the internal degrees of freedom. The cutoff energy of the product translational energy distribution is about 32 kcal/mol, which is obviously lower than the available energy of the two radical pathways: CH_3CHCH_3 (total available energy 57.7 kcal/mol) and $CH_3CH_2CH_2$ (total available energy 55.3 kcal/mol). This is not surprising since such a phenomenon has been observed before. The relative importance of the two radical channels, however, is hard to determine experimentally. From a statistical point of view, it is very likely that the CH_3-CH_2CH_2 should be more important simply because of more H atoms at the two ends of the molecule. Again, the $O(^3P)$ reaction is also energetically possible for the OH formation channel. The available energy for the two radical pathways of this channel should be about 12.3 and 9.9 kcal/mol for CH_3CHCH_3 and CH_3-CH_2CH_2, respectively. These values are much lower than the cutoff energy observed for this channel, indicating the $O(^3P)$ reaction should be, at most, a minor contribution to this channel.

From the results obtained above, the OH products are clearly forward-scattered relative the $O(^1D)$ beam direction, indicating a direct abstraction-type mechanism is likely responsible for this reaction channel. A direct abstraction-type mechanism should be a direct process in which the reaction intermediate is very short-lived. The lifetime of this reaction intermediate is probably significant shorter than the rotational period of the complex. It is also clear that this direct abstraction process should not be a collinear process, which would likely produce backward scattered OH product. This direct abstraction occurs likely at larger impact parameters. This observation is similar to the results of the $O(^1D)$ reactions with CH_4 and C_2H_6. In addition to the direct abstraction reaction mechanism, there is also another possible mechanism contributing to the OH formation process. From the measured angular distribution for the OH product, the CM angular distribution shows a large forward contribution with much of the remaining products scattering in all directions. These remaining products could be attributed to a long-lived complex mechanism that will likely produce forward−backward symmetric or isotropic product angular distribution. From the above discussions, it is likely that the OH channel occurs through multiple dynamical pathways. As mentioned in the Introduction, previous theoretical studies suggest that the OH formation channel should go through an insertion step; however, there has been no clear theoretical evidence of the existence of a direct abstraction reaction channel yet. Experimental investigations of the OH channel in the $O(^1D)$ reaction with other saturated hydrocarbon compounds (CH_4, C_2H_6, and C_3H_8) show experimental evidence that such direct abstraction channel exists. All of these results indicate that the OH formation channel in the $O(^1D)$ reaction with CH_4 and other hydrocarbons may proceed through a similar reaction mechanism. Studies of this channel at a wide range of collisional

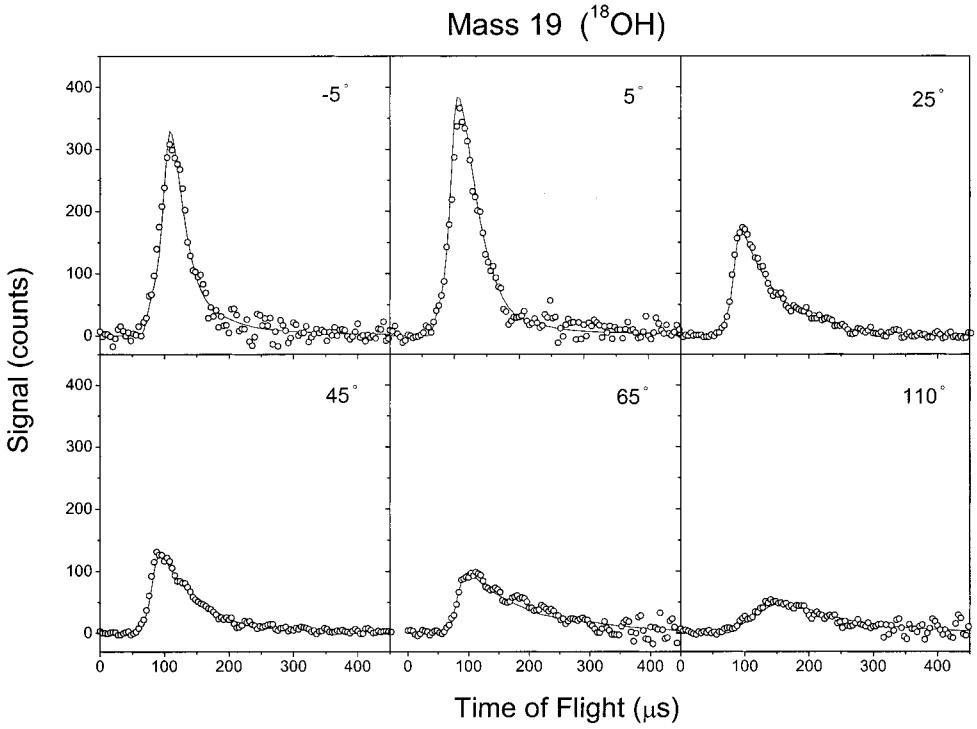

Figure 14. TOF spectra at mass 19 at 12 different laboratory angles. The Open circles represent the experimental data, while the solid lines are the simulated results. Each experimental spectrum was obtained by accumulating signals over 250K laser shots.

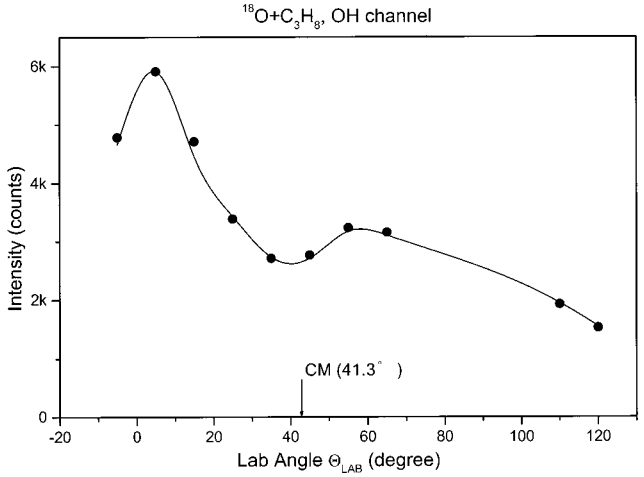

Figure 15. Laboratory angular distribution of product at mass 19. Open circles are the experimental data, while the sold line is the simulated results.

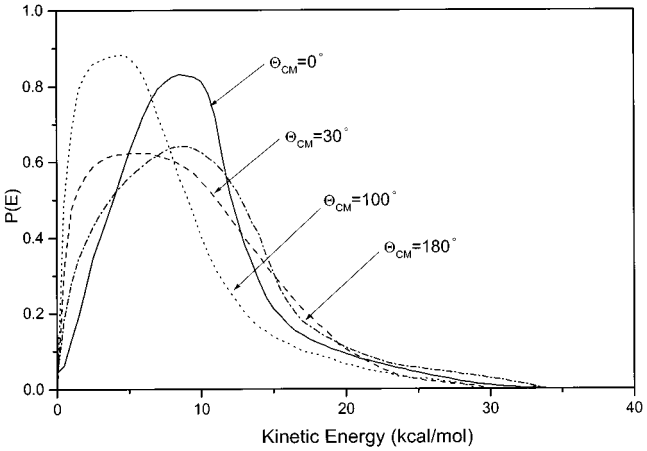

Figure 16. CM product kinetic energy distributions used in simulating the TOF spectra shown in Figure 14. Total of four distributions are used at four CM angles.

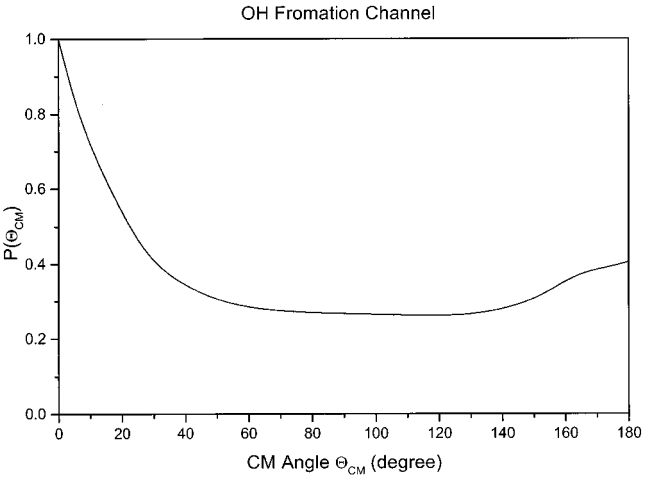

Figure 17. CM angular distribution of product observed at mass 19 obtained from simulating the TOF spectra (Figure 14) and the laboratory angular distribution (Figure 15).

energies are desirable in order to clarify the relative contributions of the direct and indirect reaction mechanisms.

3.4. Branching Ratios of Different Reaction Pathways. The relative branching ratio for the reaction channels have been determined by measuring relative signals at different masses

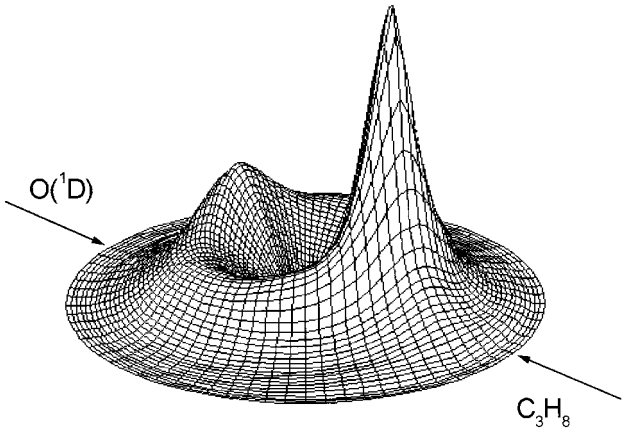

Figure 18. 3D product flux diagram for the OH product constructed from the CM product kinetic energy distributions (Figure 16) and the CM angular distribution (Figure 17).

that are detectable. Contributions from different channels to each mass are obtained by simulating all TOF spectra. In the estimation, the detection efficiencies of all of the radical products observed in this experiment are assumed to be the same because a truly quantitative characterization is not possible at this moment. The detection efficiency is the ionization efficiency multiplied by the ion transmission efficiency. This approximation works quite well for the $O(^1D) + CH_4$.[20] It is quite reasonable because the ion transmission efficiency and the ionization cross-section compensate each other in this experiment. Ion transmission efficiency decreases as product mass increases, while ionization cross-section normally increases as the product mass (also numbers of electrons in the product) increases. The relative branching ratios obtained for the four observed channels are listed in the following:

$$O(^1D) + C_3H_8 \rightarrow CH_3 + C_2H_4OH \quad 27\%$$

$$\rightarrow C_2H_5 + CH_2OH \quad 48\%$$

$$\rightarrow OH + C_3H_7 \quad 25\%$$

It is interesting to notice that the OH formation channel is actually quite more important than previous experimental results suggested.[15] It seems that at least the OH formation is a significant process in the title reaction. This could be significant when OH formation from the reactions of $O(^1D)$ with hydrocarbons is assessed in the atmosphere. As has been discussed previously, there are other possible minor channels that exist for this reaction such as the H_2O formation channel. In this experiment, no experimental evidence has been found for other reaction channels; this is probably due to the low signal levels of these channels that are likely beyond the sensitivity of our apparatus. The branching ratios provided here are quite interesting when they are compared with those of the $O(^1D) + CH_4$ reaction in which the OH formation is the dominant channel (70%) while the H formation channel is about 25% and the H_2 formation is about 5%. This picture is consistent with an insertion mechanism. Since C−C bond is weaker in the reaction complex, its cleavage should be easier than C−H bond cleavage. Therefore, the CH_3 formation channel should be more important than the other pathways.

5. Conclusions

Three different reaction channels in the $O(^1D) + C_3H_8$ reaction, the CH_3 formation, C_2H_5 formation, and the OH

formation, have been experimentally studied using the crossed molecular beam technique. Product kinetic energy distributions and angular distributions have been determined for all observed reaction channels. All three reaction channels are significant. The radical products (C_2H_5OH and CH_2OH) from the CH_3 and C_2H_5 formation channels show a forward and backward symmetric distribution, while the OH radical is strongly forward-scattered relative the $O(^1D)$ beam direction. From these experimental observations, it is quite obvious that there are different dynamical pathways for this reaction. The long-lived complex formed through insertion by the $O(^1D)$ atom seems to be the most important reaction mechanism in the title reaction, which is similar to the $O(^1D)$ reactions with CH_4 and C_2H_6. This work put together a quite complete dynamical picture for the $O(^1D) + C_3H_8$ reaction through careful crossed molecular beam investigations. This result, along with our previous results on the $O(^1D)$ reactions with CH_4 and C_2H_6, provides a series of rather complete investigations on the reactivity of the $O(^1D)$ atom with small alkane molecules.

Acknowledgment. This work is supported by the Academia Sinica, the National Science Council of the Republic of China, and the China Petroleum Co.

JA003456P